

Measurement of Radio Emission from Extensive Air Showers with LOPES

J.R. Hörandel^a, W.D. Apel^b, J.C. Arteaga^{c,n}, T. Asch^d, F. Badea^b, L. Bähren^a, K. Bekk^b, M. Bertaina^e, P.L. Biermann^f, J. Blümer^{b,c}, H. Bozdog^b, I.M. Brancus^g, M. Brüggemann^h, P. Buchholz^h, S. Buitink^a, E. Cantoni^{e,i}, A. Chiavassa^e, F. Cossavella^c, K. Daumiller^b, V. de Souza^{c,o}, F. Di Pierro^e, P. Doll^b, M. Ender^b, R. Engel^b, H. Falcke^{a,j}, M. Finger^b, D. Fuhrmann^k, H. Gemmeke^d, P.L. Ghiaⁱ, R. Glasstetter^k, C. Grupen^h, A. Haungs^b, D. Heck^b, A. Horneffer^a, T. Huege^b, P.G. Isar^b, K.-H. Kampert^k, D. Kang^c, D. Kickenbick^h, O. Krömer^d, J. Kuijpers^a, S. Lafebvre^a, K. Link^b, P. Luczak^l, M. Ludwig^c, H.J. Mathes^b, H.J. Mayer^b, M. Melissas^c, B. Mitrica^g, C. Morelloⁱ, G. Navarra^e, S. Nehls^b, A. Nigl^a, J. Oehlschläger^b, S. Over^h, N. Palmieri^c, M. Petcu^g, T. Pierog^b, J. Rautenberg^k, H. Rebel^b, M. Roth^b, A. Saftoiu^g, H. Schieler^b, A. Schmidt^d, F. Schröder^b, O. Sima^m, K. Singh^{a,p}, G. Toma^g, G.C. Trincheroⁱ, H. Ulrich^b, A. Weindl^b, J. Wochele^b, M. Wommer^b, J. Zabierowski^l, J.A. Zensus^f

^aRadboud University Nijmegen, Department of Astrophysics, P.O. Box 9010, 6500 GL Nijmegen, The Netherlands

^bInstitut für Kernphysik, Forschungszentrum Karlsruhe, Germany

^cInstitut für Experimentelle Kernphysik, Universität Karlsruhe, Germany

^dIPE, Forschungszentrum Karlsruhe, Germany

^eDipartimento di Fisica Generale dell'Università di Torino, Italy

^fMax-Planck-Institut für Radioastronomie Bonn, Germany

^gNational Institute of Physics and Nuclear Engineering, Bucharest, Romania

^hFachbereich Physik, Universität Siegen, Germany

ⁱIstituto di Fisica dello Spazio Interplanetario, INAF Torino, Italy

^jASTRON, Dwingeloo, The Netherlands

^kFachbereich Physik, Universität Wuppertal, Germany

^lSoltan Institute for Nuclear Studies, Lodz, Poland

^mDepartment of Physics, University of Bucharest, Bucharest, Romania

ⁿnow at: Universidad Michoacana, Morelia, Mexico

^onow at: Universidade de São Paulo, Instituto de Física de São Carlos, Brasil

^pnow at: KVI, University of Groningen, The Netherlands

Abstract

A new method is explored to detect extensive air showers: the measurement of radio waves emitted during the propagation of the electromagnetic shower component in the magnetic field of the Earth. Recent results of the pioneering experiment LOPES are discussed. It registers radio signals in the frequency range between 40 and 80 MHz. The intensity of the measured radio emission is investigated as a function of different shower parameters, such as shower energy, angle of incidence, and distance to shower axis. In addition, new antenna types are developed in the framework of LOPES^{STAR} and new methods are explored to realize a radio self-trigger algorithm in real time.

Key words: cosmic rays, air shower, radio emission, radio detection

PACS: 96.50.S-, 96.50.sd

1. Introduction

An intense branch of astroparticle physics is the study of high-energy cosmic rays to reveal their origin, as well as

their acceleration and propagation mechanisms [1,2,3]. At energies exceeding 10^{14} eV cosmic rays are usually studied by indirect measurements — the investigation of extensive air showers initiated by cosmic particles in the atmosphere. Different techniques are applied, like the measurements of

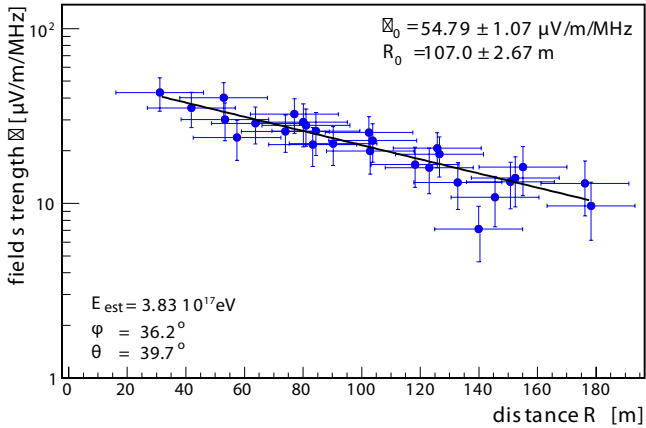


Fig. 1. Measured field strength as a function of the distance to shower axis for an individual shower [4].

particle densities and energies at ground level, or the observation of Čerenkov and fluorescence light. An alternative technique has been recently revitalized — the detection of radio emission from extensive air showers at energies exceeding 10^{16} eV.

Radio emission from air showers was experimentally discovered in 1965 at a frequency of 44 MHz [5]. The early activities in the 1960s and 1970s are summarized in [6]. Only recently, fast analog-to-digital converters and modern computer technology made a clear detection of radio emission from air showers possible. LOPES, a LOFAR Prototype Station had shown that radio emission from air showers can be detected even in an environment with relatively strong radio frequency interference (RFI) [7]. Further investigations of the radio emission followed with LOPES [8,9,10,11,12] and the CODALEMA experiment [13,14], paving the way for this new detection technique, see also [15].

The LOPES experiment registers radio signals in the frequency range from 40 to 80 MHz [16]. In this band are few strong man made radio transmitters only, the emission from air showers is still strong (it decreases with frequency), and background emission from the Galactic plane is still low. An active short dipole has been chosen as antenna. An inverted V-shaped dipole is positioned about 1/4 of the shortest wavelength above an aluminum ground plate. In this way a broad directional beam pattern is obtained. LOPES comprises 30 antennas [17] located on site of the KASCADE-Grande experiment [18,19] one of the best air shower experiments operating in the energy range between 10^{14} and 10^{18} eV. The LOPES data acquisition is triggered by large air showers registered with KASCADE-Grande. The latter measures the showers simultaneously to LOPES and delivers precise information on the shower parameters, such as shower energy as well as position and inclination of the shower axis. All antennas, including the complete analog electronics chain, have been individually calibrated with a reference radio source [20].

Most likely, the dominant emission mechanism of the radio waves in the atmosphere is radiation due to the de-

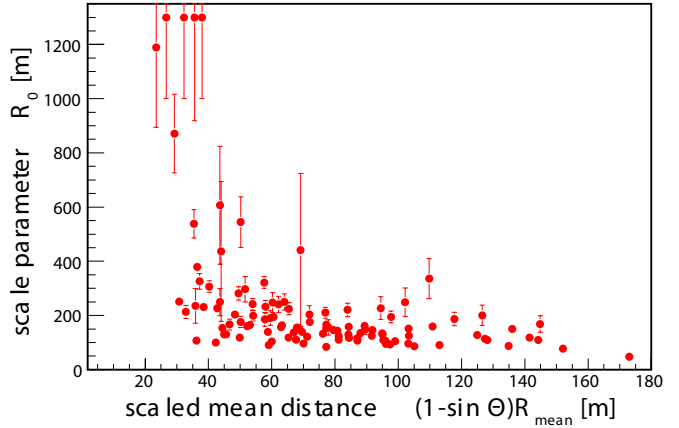


Fig. 2. Scale parameter R_0 as a function of the zenith angle times the mean distance to the shower axis [4].

flection of charged particles in the Earth’s magnetic field (geosynchrotron radiation) [21,22,23]. In the frequency range of interest the wavelength of the radiation is large compared to the size of the emission region: the typical thickness of the air shower disc is about 1 to 2 m only. Thus, coherent emission is expected which yields relatively strong signals at ground level.

2. Radio signal and shower parameters

One of the primary objectives of LOPES is to investigate the measured radio signal as a function of parameters characterizing the extensive air shower. For this purpose the shower parameters measured simultaneously with KASCADE-Grande are irreplaceable. An empirical relation has been found to express the expected east-west component of the field strength at a distance R from the shower axis as a function of shower parameters [24]

$$\epsilon = (11 \pm 1) [(1.16 \pm 0.025) - \cos \alpha] \cos \theta \exp\left(-\frac{R}{(236 \pm 81) \text{ m}}\right) \left(\frac{E_0}{10^{17} \text{ eV}}\right)^{(0.95 \pm 0.04)} \left[\frac{\mu\text{V}}{\text{m MHz}}\right]. \quad (1)$$

α is the angle between the shower axis and the direction of the Earth magnetic field (geomagnetic angle), θ the zenith angle of the shower, and E_0 the energy of the shower inducing primary particle. It is interesting to note the absolute values of some parameters: the exponential fall-off has a characteristic length of about 240 m, much larger than the classical Molière radius of electrons in air (≈ 80 m). This indicates that the lateral distribution of the radio component is flatter as compared to the electromagnetic component, an important fact to build large-scale radio arrays with an economic antenna density. The measured radio signal is almost directly proportional to the shower energy ($[0.95 \pm 0.04] \approx 1$). Such a behavior is expected for a coherent emission of the radio waves from the air showers. This calibration of the measured radio signal is a first important step towards the application of the radio detection as independent method to register extensive air showers.

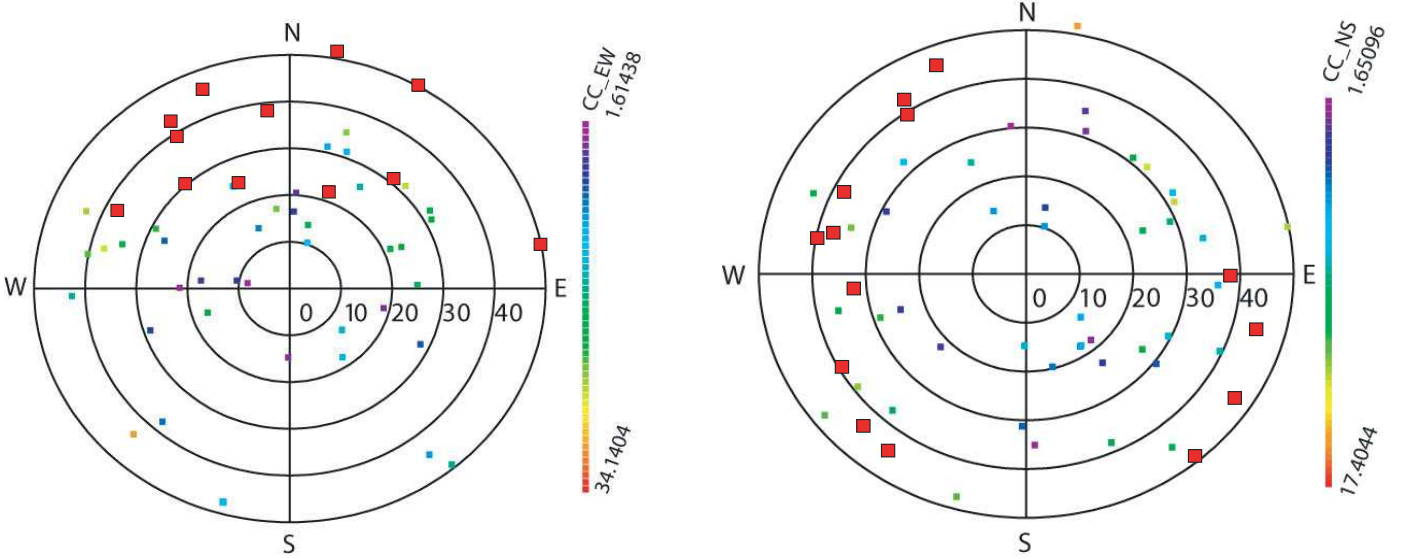


Fig. 3. Sky map of air showers detected in east-west (left) and north-south (right) polarization direction [25]. The boxes mark the arrival direction of the air showers with the strongest radio signal.

Recently, the lateral distribution of the measured radio signals has been investigated in more detail [4]. A function of the form

$$\epsilon = \epsilon_0 \exp\left(-\frac{R}{R_0}\right) \quad (2)$$

has been fitted to the measured field strength as a function of the distance to the shower axis R_0 . The measured field strength as a function of the distance to the shower axis is presented in Fig. 1 for a typical event. The characteristic length R_0 for this example is of order of 100 m.

The investigations reveal that there are different types of air showers. Most of them have a lateral distribution which is characterized by a constant $R_0 \approx 100$ to 200 m, like the example shown in Fig. 1. On the other hand, there are few showers with relatively flat lateral distributions and corresponding values for R_0 as high as 1000 m or 1200 m. A closer look indicates that the steepness of the fall-off R_0 depends on the mean distance to the shower axis R_{mean} and the zenith angle of the showers θ . The reconstructed scale parameter R_0 is plotted as a function of the relation $(1 - \sin\theta)R_{mean}$ in Fig. 2. A correlation between the two quantities can be recognized. Large values for R_0 are obtained for showers with large zenith angles and a small average distance between the shower axis the antennas. But as not all events with small R_{mean} show a flattening — the reason is still unclear and further investigations with larger statistics are required.

3. Polarization

An important contribution towards the full understanding of the emission mechanism of the radio waves in air

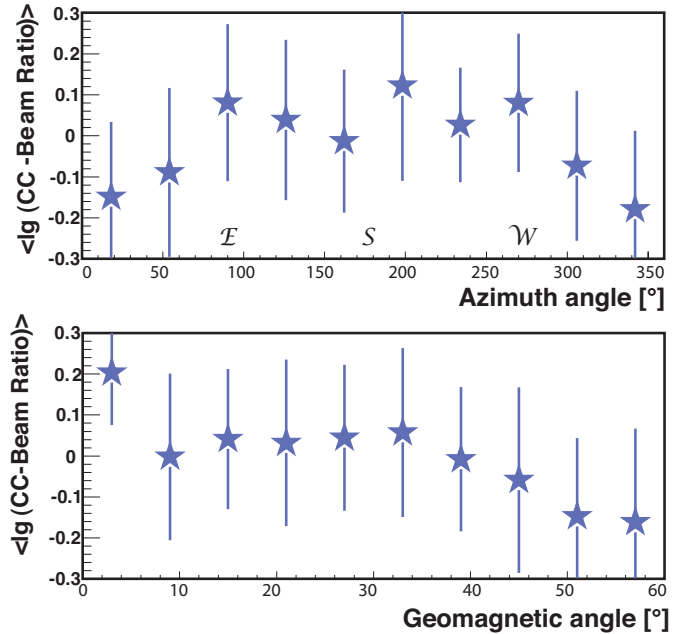


Fig. 4. Ratio of the reconstructed cross-correlated beam values of the north-south and east-west polarization components as a function of azimuth angle (top) and the geomagnetic angle (bottom) [26].

showers is the investigation of the polarization characteristics of the measured radio signals [25]. The 30 LOPES antennas are set up now such that 15 register the east-west component and 15 antennas measure the north-south component of the electric field.

The radio emission generated by the geo-synchrotron mechanism is expected to be highly linearly polarized. The signal is usually present in both polarization components (E-W and N-S). The signal strength depends on the geo-

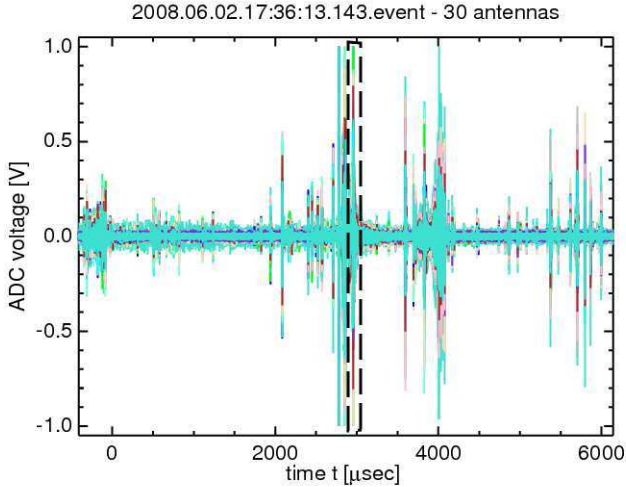


Fig. 5. Example of the measured antenna signal as a function of time for a thunderstorm event [28].

magnetic angle and thus, on the shower azimuth and zenith angles [23]. The emission is expected to be polarized perpendicular to the shower axis and the direction of the geomagnetic field. The polarization characteristics can be described by a unit polarization vector $\vec{v} \times \vec{B}$, where \vec{v} is the direction of the shower axis and \vec{B} the direction of the Earth magnetic field [26]. Recently, it has been suggested that in addition to the polarization characteristics also the absolute magnitude of the electric field is proportional to the Lorentz force $\vec{v} \times \vec{B}$ [27].

The arrival direction of the cosmic rays on the sky is shown for the registered events in Fig. 3. The color code represents the pulse heights of the cross-correlated beams, registered in east-west polarization (left) and north-south polarization (right). The boxes indicate the directions of the events with the strongest signals. The magnetic field in Karlsruhe has a zenith angle of 25° and an azimuth angle of 180° . It can be recognized that the showers with the strongest signals are registered perpendicular to the Earth magnetic field: from northern directions in east-west polarization direction and from west and east for the north-south polarized signal.

To confirm the $\vec{v} \times \vec{B}$ behavior of the polarized signals the ratio of the amplitudes of the cross-correlated beams in east-west and north-south polarization is investigated [26]. The ratio of the north-south to east-west amplitudes is depicted in Fig. 4 as a function of the azimuth angle (top) and the geomagnetic angle (bottom). Mean values and the spread of the distributions are shown. A correlation between the plotted quantities can be clearly recognized. The ratio of the north-south divided by the east-west component of the $\vec{v} \times \vec{B}$ vector of the measured showers exhibits the same behavior as a function of the azimuth angle and geomagnetic angle. This $\vec{v} \times \vec{B}$ behavior of the measured data is a strong indication for a geomagnetic origin of the radio emission in air showers.

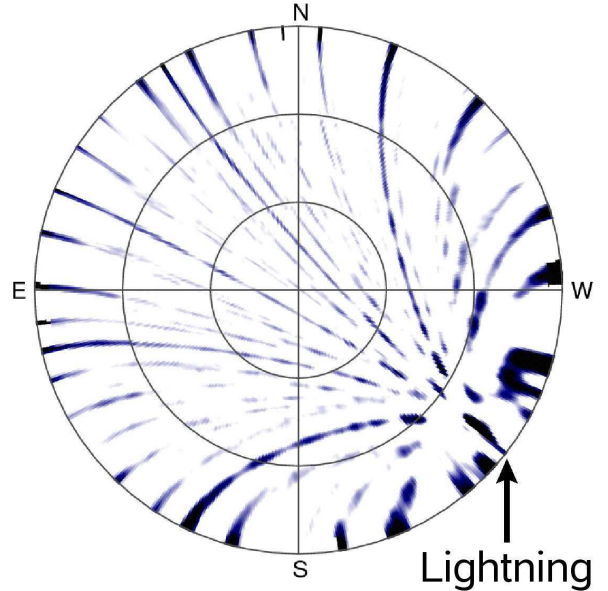


Fig. 6. Sky map of the thunderstorm event shown in Fig. 5 [28].

4. Thunderstorm events

The measured field strength of the radio emission of air showers depends on the (static) electric fields in the atmosphere. The electric fields inside thunderstorm clouds, in particular within the convective region can reach peak values up to 100 kV/m. This leads to additional forces on the electrons and positrons in the air showers and, consequently, to an acceleration and deceleration of parts of the electromagnetic shower component (electrons and positrons, depending on the direction of the electric field). In turn, this yields to an amplification or reduction of the radio emission of air showers during thunderstorms. Such a behavior has been observed with LOPES [10]. To obtain reliable information about the detected air showers from the observations of radio emission requires to monitor the electric field in the atmosphere and to record the signatures of thunderstorms. Therefore, the signals from air showers during thunderstorms are studied in detail [28].

As an example, the antenna signal as a function of time measured during a thunderstorm is shown in Fig. 5. A signal from an air shower is expected at the zero point of the time axis with an amplitude less than 0.1 V. Strong additional signals caused by lightning can be recognized. The dashed lines mark a region with strong lightning signals, which is used to calculate a sky-map of the cross-correlated beam. The result is presented in Fig. 6. The map shows the whole sky with the zenith in the center and the horizon at the border. A strong signal is visible in south-western direction, marking the discharge region of the lightning. The signal extends to the horizon. This indicates that a cloud-ground discharge has been registered (and not a cloud-cloud discharge). The grating lobes of the antenna array extend over the whole sky.

At present, studies are under way to detect a possible dis-

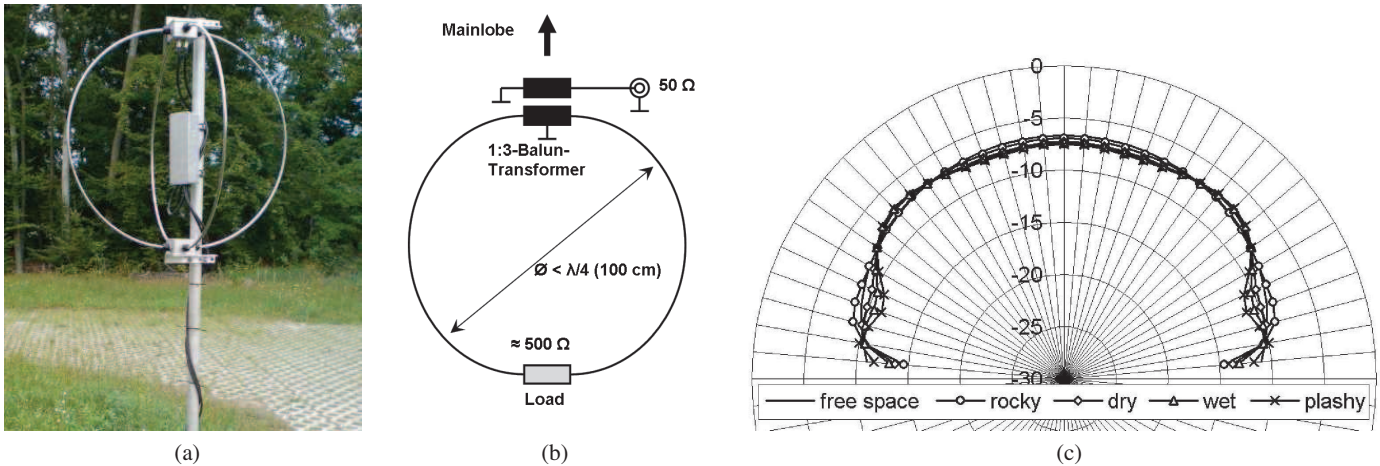


Fig. 7. Photo of a SALLA antenna and circuit diagram (left). E-plane directional diagram (right) [29].

tortion of an event due to thunderstorm conditions directly from the measured data [28]. The idea is to find a possible deviation of the polarization characteristics from the theoretically expected behavior. Such an indication would point towards a change in the emission process.

5. New antenna types and self-trigger algorithms

An important objective of LOPES is to develop and optimize new antenna types to measure radio signals from extensive air showers in large installations, such as the Pierre Auger Observatory, see Sect. 6: a sub-project named LOPES^{STAR}. Most cosmic-ray radio detectors use (simple) dipole antennas, they are easy to assemble and are available at relatively low costs. To avoid uncertainties related to dipoles new antenna types are developed, such as the logarithmic periodic dipole antenna (LPDA) with two crossed polarization directions [30]. These antennas exhibit an almost frequency independent directional diagram, antenna gain, and impedance.

Another way to design wide-band directional antennas with dimensions much smaller than the LPDA is given by resistively loaded aperiodic antennas with internal losses [29]. They also have excellent wide-band properties as the resistor load dominates in comparison to the capacitive or inductive reactance. For a large-scale radio detector a crossed polarized short aperiodic loaded loop antenna (SALLA) has been developed. It has a diameter of only 100 cm (120 cm in the latest version), a weight less than 2 kg, and material costs of about 60 EUR. A photograph of the antenna and the circuit diagram are depicted in Fig. 7. The damping resistor guarantees a wide bandwidth. The E-plane directional diagram is shown in Fig. 7 (right). It features a wide main lobe towards zenith. The 3 dB beam width amounts to 150° and is about 50° wider than the directional pattern of the LPDA.

Ultimate goal is to use these antennas in a self-triggered mode, i.e. the data acquisition is started directly from the detected radio signal [31]. A trigger algorithm has been

developed and realized in FPGA-hardware. It provides RFI suppression by Fourier transforming the radio signal to the frequency domain in real time, eliminating mono frequent carriers and transforming it back to the time domain. Then a threshold is applied and events are selected which fulfill certain criteria to characterize the pulse shape. In a last step, coincidences between three neighboring antennas are required for a valid event. The real-time feasibility of this trigger mechanism was proven on prototype hardware.

6. Outlook

The investigations of radio signals from air showers with LOPES and CODALEMA are the basis for the application of these technique in large-scale experiments. The next step is to utilize the radio detection technique in large arrays, comprising several hundreds of antennas.

LOPES serves as prototype for the detection of radio emission from air showers in LOFAR [32]. The Low Frequency Array (LOFAR) is a new digital radio observatory, presently under construction in the Netherlands and in Europe [33]. It is designed as multi-sensor network to assist scientists in the fields of astronomy, geophysics, and agriculture. Main focus of the astronomy community is to observe the radio Universe in the frequency range from 30 to 240 MHz. An objective of LOFAR is the detection of radio emission from particle cascades, originating from extremely high-energy particles from outer space. Two main lines of research are followed: (i) the measurement of radio emission from extensive air showers, generated by interactions of high-energy cosmic rays in the atmosphere [34] and (ii) the detection of radio emission of particle cascades in the Moon, originating from ultra high-energy neutrinos and cosmic rays interacting with the lunar surface [35].

More than 40 stations with fields of relatively simple antennas will work together as digital radio interferometer. The antenna fields are distributed over several countries in Europe with a dense core in the Netherlands. The latter will have at least 18 stations in an area measuring roughly

$2 \times 3 \text{ km}^2$. Each station will comprise 96 low band antennas, simple inverted V-shaped dipoles (like the LOPES antennas), operating in the frequency range from 30 to 80 MHz. Each antenna will have a dipole oriented in north-south and east-west directions, respectively. In addition, fields¹ of high-band antennas will cover the frequency range from 110 to 240 MHz. For air shower observations the signals from the low band antennas are digitized and stored in a ring buffer (transient buffer board, TBB). For valid triggers the data are sent to a central processing facility, based on an IBM Blue Gene supercomputer. First data from LOFAR are expected in early 2010.

Goal of LOFAR is to further push the development of radio detection to be a new, independent way to measure the properties of air showers. Ultimate goal is to derive information about the primary, shower-inducing particle from the measurements, such as the particles energy, mass, direction and point of incidence. The curvature of the shower front has been investigated [36,37]. It could be shown that the radius of curvature measured at ground level from the radio observations is related to the distance to the shower maximum. The depth of the shower maximum in the atmosphere X_{max} is an important observable to determine the mass of the primary particle. The study indicates a resolution of X_{max} from radio observations of order of 30 – 40 g/cm².

Another important application is the measurement of radio emission from air showers at the Pierre Auger Observatory with the Auger Engineering Radio Array (AERA) [38,39]. AERA is co-located with the infill array of the Pierre Auger Observatory and in the field of view of the high-altitude fluorescence telescopes (HEAT). This unique set-up will allow to register air showers simultaneously with three independent detection methods: radio waves, fluorescence light, and particle detection in water Čerenkov detectors. AERA comprises about 150 antennas located on an area of about 20 km² and is designed to cover the energy range from 10^{17} to 10^{19} eV. It has three main science goals: (i) the thorough investigation of the radio emission from air showers and the analysis of the observed field strength as a function of various air shower parameters, such as energy, angle of incidence, and distance to the shower axis. (ii) Exploration of the capability of the radio detection technique and to study the feasibility as stand-alone technique to measure the properties of air showers. (iii) To measure the composition of cosmic rays in the energy range from 10^{17} to 10^{19} eV. First data from AERA are expected before Summer 2010.

The radio detection of air showers is a fast growing sub-discipline in astroparticle physics. With the new experiments starting operation exciting results are expected in the next few years.

References

- [1] J. Blümer, R. Engel, J. Hörandel, Prog. Part. Nucl. Phys. (2009) in press (arXiv 0904.0725).
- [2] J. Hörandel, Adv. Space Res. 41 (2008) 442.
- [3] J. Hörandel, Rev. Mod. Astron. 20 (2008) 203.
- [4] S. Nehls, et al., Proc. 31th Int. Cosmic Ray Conf., Lodz (2009) # 417.
- [5] J. Jelley, et al., Nature 205 (1965) 327.
- [6] H. Allan, Progress in Elementary Particles and Cosmic Ray Physics, J.G. Wilson & S.G. Wouthuysen eds., North Holland, 1971, p. 169.
- [7] H. Falcke, et al., Nature 435 (2005) 313.
- [8] W. Apel, et al., Astropart. Phys. 26 (2006) 332.
- [9] J. Petrovic, et al., Astron. & Astroph. 462 (2007) 389.
- [10] S. Buitink, et al., Astron. & Astroph. 467 (2007) 385.
- [11] A. Nigl, et al., Astron. & Astroph. 488 (2008) 807.
- [12] A. Nigl, et al., Astron. & Astroph. 487 (2008) 781.
- [13] D. Ardouin, et al., Nucl. Instr. & Meth. A 555 (2005) 148.
- [14] D. Ardouin, et al., Astropart. Phys. 26 (2006) 341–350.
- [15] H. Falcke, et al., arXiv:0804.0548 (2008).
- [16] A. Horneffer, et al., Proc. of the SPIE 5500 (2004) 129.
- [17] S. Nehls, et al., Proc. 29th Int. Cosmic Ray Conf., Pune 8 (2005) 45.
- [18] T. Antoni, et al., Nucl. Instr. & Meth. A 513 (2003) 490.
- [19] G. Navarra, et al., Nucl. Instr. & Meth. A 518 (2004) 207.
- [20] S. Nehls, et al., Nucl. Instrum. Meth. A589 (2008) 350.
- [21] T. Huege, H. Falcke, Astron. & Astroph. 412 (2003) 19.
- [22] T. Huege, H. Falcke, Astron. & Astroph. 430 (2005) 779.
- [23] T. Huege, H. Falcke, Astropart. Phys. 24 (2005) 116.
- [24] A. Horneffer, et al., Proc. 30th Int. Cosmic Ray Conf., Merida 4 (2008) 83.
- [25] P.G. Isar, et al., Nucl. Instr. & Meth. A (2009) in press.
- [26] P.G. Isar, Proc. 31th Int. Cosmic Ray Conf., Lodz (2009) # 1128.
- [27] D. Ardouin, et al., Astropart. Phys. 31 (2009) 192.
- [28] M. Ender, et al., Proc. 31th Int. Cosmic Ray Conf., Lodz (2009) # 405.
- [29] O. Krömer, et al., Proc. 31th Int. Cosmic Ray Conf., Lodz (2009) # 1232.
- [30] H. Gemmeke, et al., Acoustic and Radio EeV Neutrino Detection Activities, R. Nahnauer, S. Böser eds., World Scientific, 2005, p. 242.
- [31] A. Schmidt, et al., Proc. 31th Int. Cosmic Ray Conf., Lodz (2009) # 1124.
- [32] J. Hörandel, et al., Nucl. Phys. B (Proc. Suppl.) (2009) in press.
- [33] LOFAR, www.lofar.org (2009).
- [34] A. Horneffer, et al., Proc. 31th Int. Cosmic Ray Conf., Lodz (2009) # 369.
- [35] K. Singh, et al., Proc. 31th Int. Cosmic Ray Conf., Lodz (2009) # 1077.
- [36] S. Lafèbre, et al., submitted to Astropart. Phys. (2008).
- [37] S. Lafèbre, et al., Proc. 31th Int. Cosmic Ray Conf., Lodz (2009) # 587.
- [38] R. Dallier, these proceedings.
- [39] A. van den Berg, et al., Proc. 31th Int. Cosmic Ray Conf., Lodz (2009) # 232.

¹ The fields comprise 48 antennas in the Dutch stations and 96 in the European ones.